Summertime soil hydrological cycle and surface energy balance on the Mongolian steppe

T. Yamanaka[a],*, I. Kaihotsu[b], D. Oyunbaatar[c], T. Ganbold[c]

[a]*Terrestrial Environment Research Center, University of Tsukuba, Tsukuba 305-8577, Japan*
[b]*Department of Natural Environmental Sciences, Hiroshima University, Higashi-Hiroshima 739-8521, Japan*
[c]*Institute of Meteorology and Hydrology, Ulaanbaatar-46, Mongolia*

Abstract

We conducted combined measurements of soil water balance and surface energy fluxes at four sites within the Mongolian steppe region during the summer of 2001 to investigate the present state of the soil hydrological cycle, surface energy balance, and the role of vegetation in those processes. The summer total precipitation comprised 71–91% of the annual total ($= 100 \pm 6$ mm) at the sites, and was approximately equal to summer total evapo-transpiration. Moreover, the net infiltration flux was always balanced by changes in water storage within the uppermost 20 cm of the soil layer, suggesting that very little percolation occurs to depths in excess of 20 cm. The mean residence time of water stored within the layer is estimated to range from 20 to 25 days during summer. We observed a strong linear relationship (correlation coefficients ranging from 0.72 to 0.85) between latent heat flux (lE) and water-content at 3 cm depth (θ_3). The ratio of the lE change to the θ_3 change increases with increasing vegetation cover. This fact indicates that steppe vegetation helps to drive the observed rapid water cycle, and controls the surface energy balance via a strong constraint on lE.
© 2006 Elsevier Ltd. All rights reserved.

Keywords: Soil water balance; Land–atmosphere interaction; Energy budget; Semi-arid grassland; Ecotone

1. Introduction

The Mongolian steppe region is situated within an ecological transition zone (i.e. ecotone), with a strong climate gradient between the Gobi Desert to the south and the

*Corresponding author. Tel.: +81 29 853 2538; fax: +81 29 853 2530.
E-mail address: tyam@suiri.tsukuba.ac.jp (T. Yamanaka).

Siberian taiga to the north. The ecotone is highly vulnerable to future scenarios of climate change such as global warming (Roberts, 1994), especially as northeast Asia has one of the strongest warming signals on earth (Hansen et al., 1999; Chase et al., 2000).

The region is further at risk of desertification resulting from human activity (Sneath, 1998). Numerical experiments indicate that desertification in the Mongolian steppe region will act to reduce rainfall over and around the region through modification of the surface energy balance (Xue, 1996). In fact, summertime precipitation over the region has shown a significant decrease since the mid-1950s (Yatagai and Yasunari, 1995). Although there remain uncertainties with regard to whether the trend is human-induced or natural, a decrease in precipitation may naturally accelerate further desertification because the storage of soil moisture strongly regulates both vegetation activity (Kondoh and Kaihotsu, 2003; Miyazaki et al., 2004) and biodiversity (Ni, 2003) in the region.

Most of the Mongolian steppe region is located within a large internal drainage basin (the Central Asian Internal Drainage Basin; Batnasan, 2003), within which perennial rivers are either nonexistent or terminate in interior land-locked basins. For this hydro-geographical situation, we can expect that precipitated water will result in little discharge to rivers or ground-water: water exchange between grassland and the atmosphere through precipitation and evapo-transpiration is the main branch of the hydrological cycle. Thus, changes in the soil–hydrological balance resulting from climate change may have dramatic effects on the water resources stored within the region (Bradley, 1999, p. 310).

Water and energy exchanges between the terrestrial biosphere and the atmosphere are important not only in arid/semi-arid regions but also all over the globe (Betts et al., 1996); consequently, large-scale field experiments have been planned and executed under various climatic settings (Sellers et al., 1997). There are, however, few observational studies that link the soil hydrological cycle and the surface energy balance within desert-like ecosystems. This lack of information is partly due to difficulties in obtaining accurate ongoing measurements of water/energy fluxes and storage under severe weather conditions. Consequently, we lack the observational data necessary to understand interactions between the hydrological cycle, climate, and vegetation under considerably arid conditions and to test or improve numerical models used to assess the impacts of global warming on desertification and/or water resources.

In the present study, we conducted combined measurements of soil water balance and surface energy fluxes during the summer of 2001 at four sites within the Mongolian steppe region. The objectives of the study are: (1) to reveal the present state of the soil hydrological cycle in the region; (2) to assess the effect of transient soil-moisture conditions on energy fluxes under an arid climate; and (3) to understand the role of steppe vegetation in water/energy exchanges between the land surface and the atmosphere.

2. Materials and methods

2.1. Study area and field monitoring

Under the framework of the ADEOS II Mongolian Plateau Experiment for Ground Truth (AMPEX; Kaihotsu et al., 2002), Automatic Weather Stations (AWS) were deployed at four sites (Mandalgobi (MGS), Dergertsogt (DGS), Deren (DRS), and Bayantsagaan (BTS); Table 1; Fig. 1) in central Mongolia for soil–hydrological and micrometeorological monitoring. A number of ephemeral river channels occur within the

Table 1
Description of study sites

Site	Latitude	Longitude	Altitude (m)	Vegetation cover[*]	Mean grass height[*] (cm)
Mandalgobi (MGS)	45°44′35″N	106°15′52″E	1384	0.15	3.0
Delgertsogt (DGS)	46°07′38″N	106°22′07″E	1411	0.30	2.5
Deren (DRS)	46°12′31″N	106°42′53″E	1312	0.30	4.5
Bayantsagaan (BTS)	46°46′35″N	107°08′32″E	1377	0.20	5.0

[*]Measured on 8–10 June 2001.

Fig. 1. Study area (denoted as a gray box) and location of automatic weather stations (AWS; denoted as open circles insides the box). Site descriptions are provided in Table 1.

study area, and playa lakes form temporarily following heavy rainfall events. Annual precipitation is approximately 100–150 mm, with summertime precipitation generated by thermal convection and frontal storms making up most of the annual total. The topography of the area comprises rolling hills within the altitude range of 1200–1600 m. The soil at all sites is sandy loam or sandy silt loam with abundant gravel, and vegetation is dominated by *Stipa* spp., *Carex* spp., *Cleistogenes* spp., *Artemisia* spp., and *Allium tenuissimum*.

Table 2 summarizes those components that are continuously monitored by AWS. All measured values were recorded by a data logger (CR10X, Campbell Scientific Inc., USA) at 30-minute intervals. A coupled thermometer and humidity sensor was installed within a double radiation shield. A ventilation fan was used for 3 min prior to measurement in order to reduce the radiative heating/cooling of the sensors. The upper and lower polyethylene domes of the net radiometer were also ventilated to reduce their radiative heating/cooling and to combat the formation of dew on the dome surface. An infrared radiation thermometer was set to a south-west direction with a view angle approximately 45° off nadir. All above-ground sensors were mounted on a mast of 3 m in height. Soil thermometers and time domain reflectometry (TDR) sensors were inserted horizontally at four depths. Temperature effects on soil bulk dielectric permittivity (Wraith and Or, 1999)

Table 2

Summary of components monitored by the automatic weather stations at the four sites

Component	Instrument	Sampling interval	Height (m)			
			MGS	DGS	DRS	BTS
Air temperature	Ventilated platinum resistance thermometer (C-PT-10, Climatec Inc., Japan)	10 min	1.60	1.50	1.50	1.50
Relative humidity	Ventilated capacitance humidity sensor (50Y, Vaisala Oy, Finland)	10 min	1.60	1.50	1.50	1.50
Surface temperature	Infrared radiation thermometer (4000-4GL, Everest Interscience Inc., USA)	10 sec	1.50	1.45	1.40	1.45
Soil temperature	Platinum resistance thermometer (C-PTWP-5, Climatec Inc., Japan)	30 min	−0.03 −0.1 −0.4 −1.0	−0.03 −0.1 −0.4 −1.0	−0.03 −0.1 −0.4 −1.0	−0.03 −0.1 −0.2 −0.4
Soil water content	Time domain reflectometer (Trime-IT, IMKO Micromodultechnik Gmbh, Germany)	30 min	−0.03 −0.1 −0.4 −1.0	−0.03 −0.1 −0.4 −1.0	−0.03 −0.1 −0.4 −1.0	−0.03 −0.1 −0.2 −0.4
Precipitation	Tipping bucket rain gauge (7856 M, Davis Instruments, USA)	30 min	1.15	1.05	1.00	1.10
Air pressure	Barometer (PTB100B, Vaisala Oy, Finland)	30 min	1.10	1.10	1.00	1.10
Wind speed	Propeller anemometer with wind vane (05103-47, R.M. Young Company, USA)	10 sec	3.20	3.20	3.20	3.20
Wind direction	Wind vane (05103-47, R.M. Young Company, USA)	10 sec	3.20	3.20	3.10	3.15
Net radiation	Net radiometer (Q*7, REBS Inc., USA)	30 min	1.50	1.40	1.40	1.50
Heat flux	Soil heat flux plate (PHF-01, REBS Inc., USA)	10 sec	−0.05	−0.05	−0.05	−0.05

measured by TDR were corrected using an empirical model based on temperature, water-content, and soil texture parameters (Yamanaka et al., 2003).

Although field monitoring has been ongoing since August 2000, data for the summer (June–July–August; JJA) of 2001 was used to analyze the water and energy balance. The reasons for this are three-fold: (1) TDR measurement is affected by soil freezing/melting in spring and autumn and these errors are not easily corrected; (2) the accuracy of sensible heat flux measurements undertaken in winter is relatively poor because the atmospheric stability is so strong that it is difficult to correct for this effect; and (3) the reliability of

measured surface temperature as a spatially representative value decreased during the summer of 2002 because of changes in vegetation conditions surrounding the AWS.

2.2. Calculation of water and energy fluxes

Assuming minimal surface runoff, the net infiltration flux I (kg/m^2/s) is simply given as

$$I = P - E, \tag{1}$$

where P (kg/m^2/s = mm/s) is precipitation and E (kg/m^2/s) is the evapo-transpiration flux (or dew flux in the case of a negative sign). P was measured using a tipping bucket raingauge, and E was calculated from the surface energy balance expressed as

$$E = (R_n - G - H)/l, \tag{2}$$

where R_n (W/m^2) is net radiation, G (W/m^2) is the soil heat flux, H (W/m^2) is the sensible heat flux, and l (J/kg) is the latent heat of water for evaporation. Multiplying E by l gives the latent heat flux, lE (W/m^2). R_n was measured directly using a net radiometer, and G was obtained from a combination of heat-flux-plate measurements and soil calorimetry between the plate and the soil surface (Brutsaert, 1982, pp. 149–150).

The sensible heat flux was computed using the bulk-transfer equation with stability correction:

$$H = \frac{k u_* \rho c_p (T_s - T_a)}{\ln(z_T/z_{0h}) - \Psi_h}, \tag{3}$$

where k is von Kármán's constant (= 0.4), u^* (m/s) is the friction velocity, ρ (kg/m^3) is the density of air, c_p (J/kg/K) is the specific heat of air for constant pressure, T_s (°C) is the surface temperature, T_a (°C) is the air temperature, z_T (m) is the measurement height for air temperature, z_{0h} (m) is the roughness length for sensible heat (= z_0/10 for grassy surfaces; where z_0 (m) is the roughness length), and ψ_h is the stability correction function for sensible heat u^* is given by

$$u^* = \frac{k u}{\ln(z_u/z_{0m}) - \Psi_m}, \tag{4}$$

where u (m/s) is wind velocity, z_u (m) is the measurement height for wind velocity, z_{0m} (m) is the roughness length for the momentum (= z_0 except for very smooth surfaces), and ψ_m is the stability correction function for the momentum. Since both ψ_h and ψ_m are functions of H and u^* (Brutsaert, 1982, pp. 68–71), iterative calculations of H, u^*, and the stability correction functions were conducted until convergence values were obtained. In this study, z_0 was given by the product of the vegetation cover and the mean grass height.

The method used in this study is not a Bowen ratio-energy balance (BREB) method, which is a more common method applicable to arid/semi-arid environments (e.g. Malek and Bingham, 1993). The advantages of the present method include the use of a greater temperature difference (i.e. T_s–T_a) than that used in the BREB method and the fact that there is no requirement to measure the humidity gradient, which is usually very small under an arid climate. The main disadvantage of our method is that errors in measurements of H, R_n, and G are accumulated and reflected in lE. We adopted the present method because of the ease of maintenance and the low cost of instrumentation. In general, the relative error in E measured by micrometeorological methods (including the

present method and BREB method) is approximately $\pm 10\%$ (Scanlon et al., 1997). This error is almost twice the error for P (i.e. $\pm 5\%$).

2.3. Evaluation of soil water storage and residence time

Water storage in a soil column with the unit ground-surface area S (mm) can be evaluated by summing the water storage in each sub-layer:

$$S = \sum_{i=1}^{n} (\theta_{\mathrm{u}}^i + \theta_{\mathrm{l}}^i) d^i / 2, \tag{5}$$

where θ_{u}^i and θ_{l}^i (m^3/m^3) are the volumetric water-content at the upper and lower boundaries of the ith sub-layer, respectively; d^i (mm) is the thickness of the layer; and n is the number of sub-layers. As the top layer θ_{u}^1 cannot be measured by TDR, we assumed $\theta_{\mathrm{u}}^1 = \theta_{\mathrm{l}}^1$.

If the change in S is balanced by the net infiltration flux, there is no deep percolation through the bottom of the soil column, suggesting that all the precipitated waters return into the atmosphere via evapo-transpiration. In this case, the mean residence (or turnover) time of water in the column, τ (day), can be evaluated from

$$\tau = \frac{S_{\mathrm{m}}}{P_{\mathrm{m}}} \tag{6}$$

where S_{m} (mm) is the mean water storage in the soil column for a given period and P_{m} (mm/day) is the mean precipitation for the same period. τ provides a measure of the timescale of the soil-hydrological cycle within the study region.

3. Results and discussion

3.1. Hydro-meteorological conditions

Table 3 summarizes the hydro-meteorological conditions for the year from September 2000 to August 2001 or during the last 3 months of the period (i.e. period of the analysis). Annual mean air temperature was approximately zero and was slightly dependent on the latitude and altitude of the monitoring site. The annual range in air temperature exceeded $40\,^\circ$C for all sites. Monthly mean air temperature and soil temperature were less than $0\,^\circ$C during the period from October to the following March. Even during September, April, and May, instantaneous values of air and soil temperatures fell below the freezing point.

Annual mean net radiation and annual total precipitation were approximately 60 W/m^2 and 100 mm, respectively. Budyko's radiational index of dryness ($\equiv R_{\mathrm{n}}/lP$) is much higher than 3, suggesting that this area is classified as desert in a climatic sense. The total precipitation during JJA comprised 71–91% of total annual precipitation; for months other than JJA, mean monthly precipitation is less than 3 mm. The average JJA volumetric water-content at 3 cm depth ranged from 1.3% to 8.2% among the sites; spatial differences may depend on soil retention properties and/or the gravel content around TDR sensors. Temporal variations in soil water-content at 40 cm and 1 m depths were not significant except for an apparent change in TDR output related to soil freezing/melting. Relative humidity ranged from 41% to 48% and is not correlated with precipitation or soil water-content.

Table 3
Summary of hydro-meteorological conditions during the year from September 2000 to August 2001 (or June–July–August 2001) at the four sites

Site	T_{ave} (°C)	T_{max} (°C)	T_{min} (°C)	Rn (W/m^2)	P (mm)	P_{JJA} (mm)	θ_{JJA} (%)	RH_{JJA} (%)
MGS	2.3	21.5	−19.8	59.5	107.4	97.5	8.2	41.1
DGS	0.9	20.2	−22.2	62.2	102.6	77.3	1.3	47.8
DRS	1.3	21.5	−23.9	57.6	101.2	71.8	7.3	41.7
BTS	−0.1	20.5	−22.4	58.5	90.2	69.0	3.8	45.8

T_{ave}, annual mean air temperature; T_{max}, maximum monthly mean air temperature; T_{min}, minimum monthly mean air temperature; Rn, annual mean net radiation; P, annual total precipitation; P_{JJA}, total precipitation during June–July–August; θ_{JJA}, mean volumetric water content at a 3-cm depth during June–July–August; RH_{JJA}, mean relative humidity during June–July–August.

Although both annual and summer precipitation was greater in the south-west than the northeast, this trend is occasional rather than common. Spatial variations in the other measured hydro-meteorological conditions are also weak. In summary, spatial variations among the sites within the present study area appear to be insignificant across a scale of 100 km.

3.2. Soil hydrological balance and residence time

The total precipitation and evapo-transpiration for the 3 months are almost identical; thus, cumulative infiltration flux shows neither increasing nor decreasing trends (Fig. 2). The total infiltration during JJA was 7.0 mm for MGS, −11.4 mm for DGS, −8.1 mm for DRS, and 3.2 mm for BTS. This variation among sites is less than the sum of errors in P (± 4 mm) and E (± 8 mm). Fig. 2 also displays soil moisture storage within the top soil layer to a depth of 20 cm (S_{0-20}), as computed by Eq. (5) using water-content at depths of 3, 10, and 20 cm. In this computation, soil moisture data at 20 cm depth for MGS, DGS, and DRS were not available; consequently, we used data at 40 cm depth as an approximate value. The measured variation in S_{0-20} correspond closely to that for cumulative infiltration. This correspondence demonstrates that the water flux (and thus the energy flux) evaluations are sufficiently reliable and that precipitated water never infiltrates to depths in excess of 20 cm. In other words, only soil moisture in the top layer takes part in water exchange between grassland and the atmosphere.

Estimates of infiltration flux from various arid settings around the world (Scanlon et al., 1997) indicate that a negligibly small amount of deep percolation is commonly found within natural vegetation areas that record annual precipitation of less than 300 mm. Working in a sparsely vegetated desert valley where annual P is approximately 160 mm, Malek et al. (1997) found that temporal variations in cumulative evapo-transpiration measured by the BREB method are very similar to variations in cumulative precipitation. Thus, the present results appear to be quite reasonable: evapo-transpiration is approximately equal to precipitation, and deep percolation is negligibly small on the Mongolian steppe, at least during summer. However, it is possible that evapo-transpiration from grassy area around playas (Malek et al., 1990) or from desert riparian zones (Si et al., 2005) exceeds precipitation. Transient, concentrated recharge to ground-water can occur via distinct
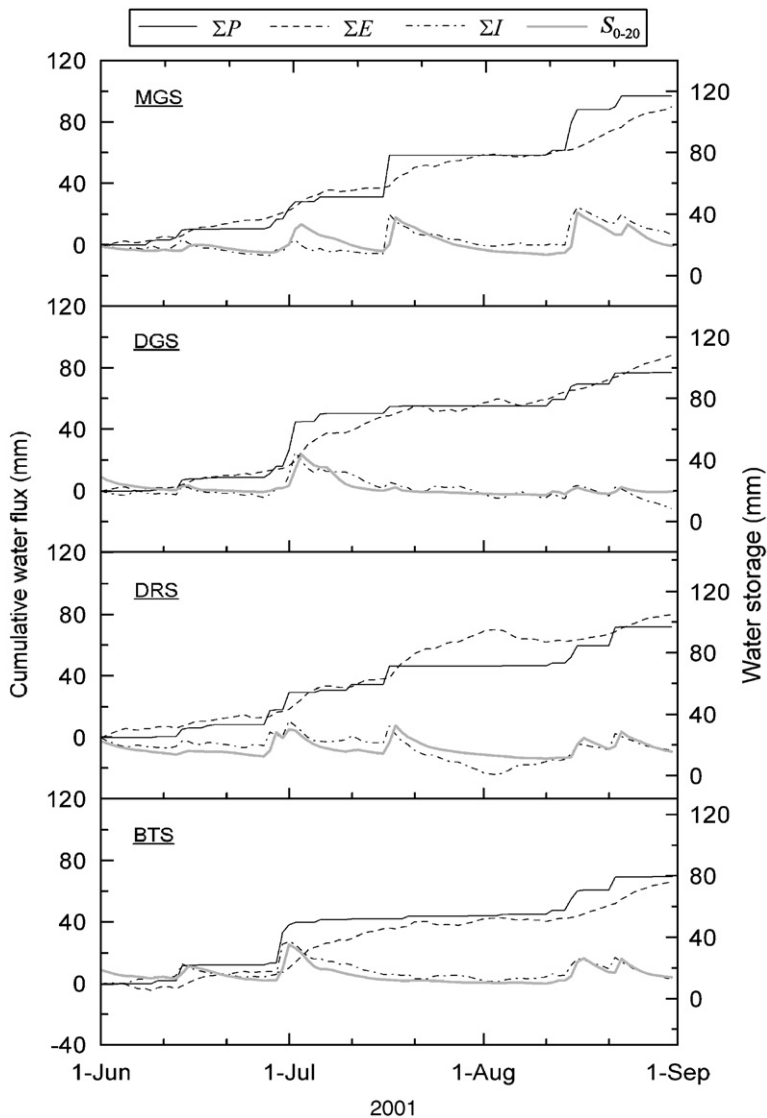
Fig. 2. Temporal evolution of cumulative precipitation (ΣP), evapo-transpiration (ΣE), and infiltration (ΣI) at the four measurement sites. Also shown is soil moisture storage in the surface layer to a depth of 20 cm (S_{0-20}).

pathways such as fractured rock or ephemeral streambeds even under an extremely arid climate (Gee and Hillel, 1988; Scanlon et al., 1997). We do not reject the possibility that concentrated discharge or recharge areas may exist in the present study region.

Malek and Bingham (1993) reported that the net infiltration flux (i.e. P–E) within an alfalfa field in Utah, USA, is balanced by changes in water storage in the upper 1 m of soil; however, to our knowledge, no previous study has reported that infiltration is balanced by changes in water storage within only the uppermost 20 cm of the soil layer. Such a result may be unique to the Mongolian steppe.

Table 4
Mean summertime water storage, flux, and residence time during at the four measurement sites

Site	S_m (mm)	P_m (mm/day)	τ (days)
MGS	21.6	1.06	20.4
DGS	21.9	0.84	26.1
DRS	17.9	0.78	22.9
BTS	15.8	0.75	21.1

S_m, mean water storage within the surface soil layer per unit area; P_m, mean precipitation; τ, mean residence time of surface soil moisture.

Here, we examine the timescale of the soil-hydrological cycle. The value of τ for JJA, as evaluated from Eq. (6) using the mean value of S_{0-20}, ranges from 20 to 26 days among the four AWS sites (Table 4), suggests that precipitated water on the grassland quickly returns to the atmosphere via evapo-transpiration. This short residence time introduces a greater variability in soil moisture and is probably a cause of the observed strong dependence of vegetation growth on soil moisture (Kondoh and Kaihotsu, 2003; Miyazaki et al., 2004). However, soil water at greater depths is expected to have a very long residence time because it is separated from the "active" hydrological cycle. To estimate the residence time of deep soil water or ground-water, it would be necessary to use an alternative approach such as an isotopic tracer approach (e.g. Allison et al., 1994).

3.3. Surface energy balance and soil moisture

Fig. 3 shows temporal variations in the energy balance components and daily precipitation at the four sites. The energy flux data are plotted as 5-day moving averages to remove random errors and to emphasize systematic variations. The latent heat flux was generally a minor component of the energy balance, increasing in response to rainfall events and in some cases exceeding the sensible heat flux. On average over the period JJA at the four sites, G, H, and lE shared 6%, 73%, and 21% of R_n, respectively. These percentages are similar to those recorded at desert playas by Malek et al. (1990) and Malek (2003), while lE from relatively moist grassland is generally the major component, being approximately three-times greater than H (Betts et al., 1996).

Temporal variations in lE are very similar to variations in surface soil moisture measured at 3 cm depth, θ_3 (Fig. 4). Strong, positive correlations between lE and θ_3 are found at all sites (Table 5). Both H and G show negative correlations with θ_3 and positive correlations with R_n. It is surprising that the correlation between lE and R_n is not statistically significant for any of the sites. Various evaporation models explicitly involve the combined effect of atmospheric factors and soil-moisture conditions (e.g. Shuttleworth, 1991), and for grassland areas many studies have reported a relationship between soil moisture and lE normalized by available energy (i.e. R_n–G) or its alternatives (e.g. Davies and Allen, 1973; Nichols and Cuenca, 1993; Crago, 1996; Brutsaert and Chen, 1996; Monteny et al., 1997). However, the results of the present study indicate that the latent heat flux is controlled almost solely by surface soil moisture rather than the combined effect of atmospheric factors and soil moisture. This probably reflects the extremely arid climate ($R_n/lP > 3$) of the study region.
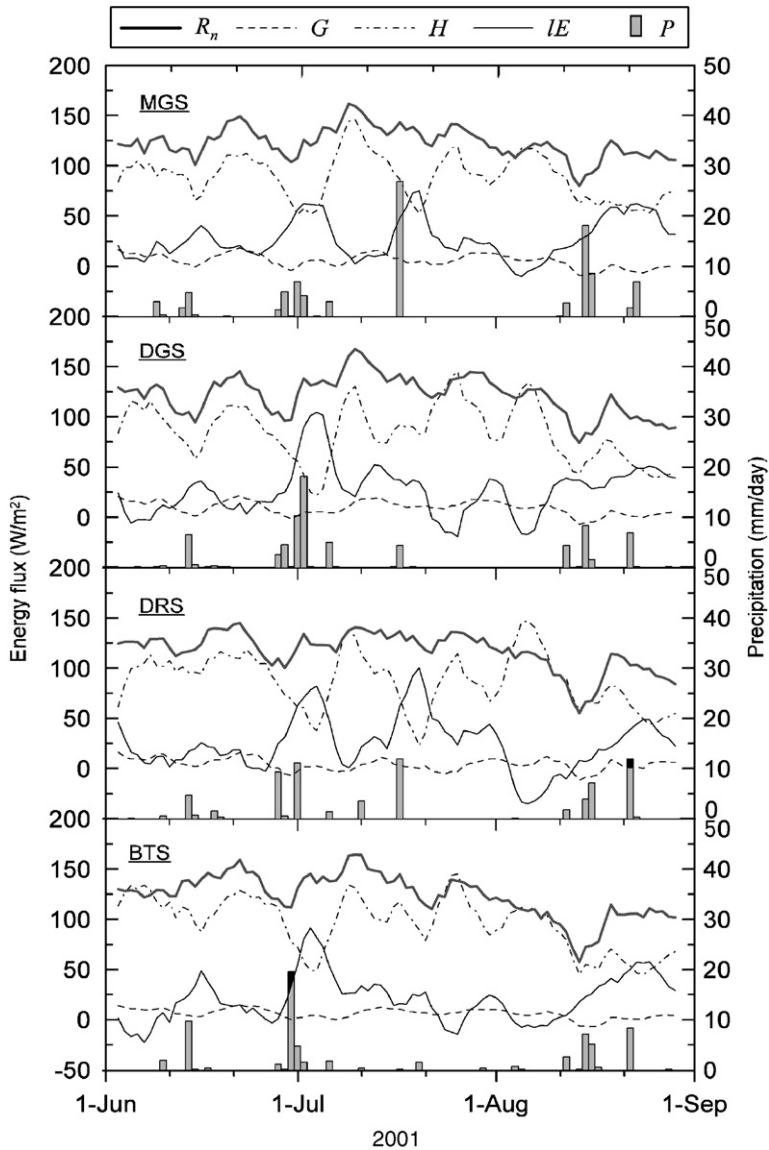
Fig. 3. Temporal variations in net radiation (R_n), soil heat flux (G), sensible heat flux (H), and latent heat flux (lE) measured at the four sites. Data are five-day moving averages. Daily precipitation (P) is also shown by bars.

The slope of the regression line between lE and θ_3 (i.e. $\Delta lE/\Delta\theta_3$) increases with increasing vegetation cover at the site (Fig. 5). This demonstrates that the latent heat flux becomes increasingly sensitive to soil moisture with the existence of vegetation. In other words, steppe vegetation aids in driving the observed rapid water exchange between the land surface and the atmosphere, and controls the surface energy balance via a strong constraint on transpiration.
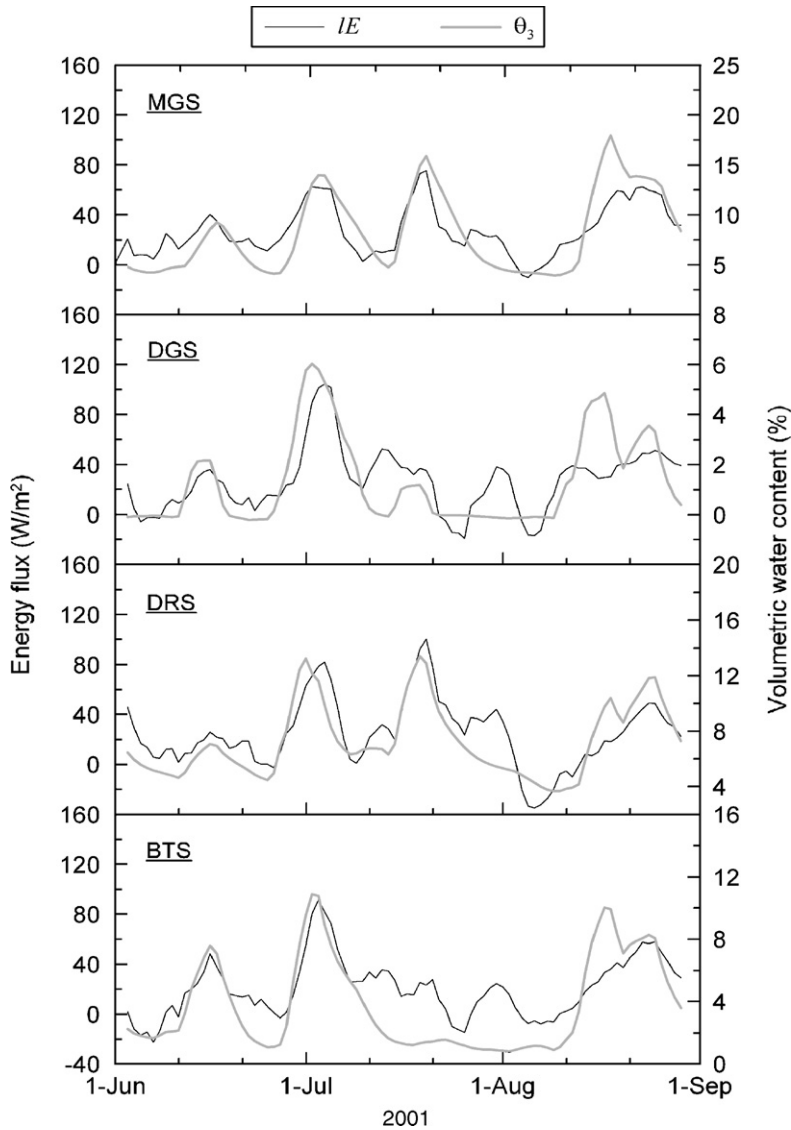
Fig. 4. Comparison of temporal variations in the latent heat flux (lE) and the soil water-content at a depth of 3 cm (θ_3) as measured at the four sites. Data are five-day moving averages.

4. Conclusions

We investigated the soil hydrological cycle, surface energy balance, and the role of steppe vegetation in the water/energy balance of the Mongolian steppe. The study period was limited to three summer months, during which time the total precipitation ranged from 71% to 91% of the annual total ($= 100 \pm 6$ mm). Differences in monitoring results among the four sites are relatively small, such that we were able to capture the common

Table 5
Correlation coefficient among 5-day moving averages of the soil water content and energy balance components

	$\theta_{3\,cm}$	R_n	G	H
(a) MGS				
Rn	−0.10			
G	−0.64***	0.64***		
H	−0.64***	0.63***	0.61***	
LE	0.85***	−0.15	−0.52***	−0.84***
(b) DGS				
Rn	−0.39***			
G	−0.79***	0.78***		
H	−0.72***	0.59***	0.64***	
lE	0.72***	−0.08	−0.37***	−0.85***
(c) DRS				
Rn	−0.06			
G	−0.47***	0.43***		
H	−0.74***	0.39***	0.29**	
LE	0.81***	0.21	−0.22*	−0.80***
(d) BTS				
Rn	−0.18			
G	−0.72***	0.64***		
H	−0.71***	0.61***	0.70***	
lE	0.79***	0.08	−0.42***	−0.73***

$\theta_{3\,cm}$, soil water content at 3 cm depth; *Rn*, net radiation; *G*, soil heat flux; *H*, sensible heat flux; *lE*, latent heat flux.
*$p<0.05$; **$p<0.01$; ***$p<0.001$.

and unique features of the Mongolian steppe region. The main findings of our study are summarized as follows:

(1) During the period June–August, the total evapo-transpiration is approximately equal to the total precipitation. Moreover, the net infiltration flux is balanced by changes in water storage within the uppermost 20 cm of the soil layer, suggesting that no (or only negligibly) deep-infiltration exists in the region, at least within relatively flat grassland during summer.
(2) The mean residence time of shallow soil moisture ranges from 20 to 26 days; that is, the precipitated water returns to the atmosphere over a considerably short time-scale. This rapid soil-hydrological cycle appears to promote greater variability in soil moisture and potentially regulates vegetation growth.
(3) On average during the summer period at the four sites, sensible heat, latent heat, and soil heat fluxes shared 73%, 21%, and 6% of net radiation, respectively. The partitioning of radiative energy into surface heat fluxes is strongly regulated by surface moisture conditions. We observed a strong linear relationship between latent heat flux and water-content at 3 cm depth, whereas the correlation between latent heat flux and net radiation was not statistically significant at any of the sites, indicating that day-to-day variation in latent heat flux is controlled almost solely by soil moisture conditions, irrespective of radiation input.
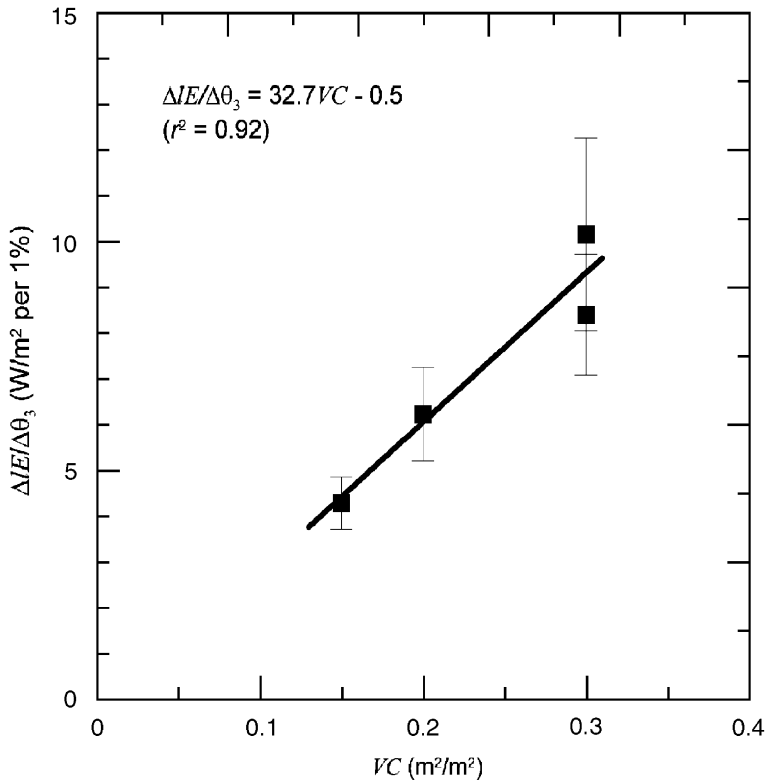
Fig. 5. Slope of the regression line between lE and θ_3 (i.e. $\Delta lE/\Delta\theta_3$) for each of the sites as a function of vegetation cover (VC) at the site. θ_3 is represented as volumetric water-content (%). Vertical bars indicate the 95% confidence intervals.

(4) The ratio of the latent heat flux change to the surface soil moisture change increases with increasing vegetation cover. This observation indicates that steppe vegetation aids in driving the rapid hydrological cycle and controls the surface energy balance via a strong constraint on transpiration.

Further investigations are required to determine inter-annual variation in water/energy fluxes and the possible effects of snowmelt on the springtime water/energy balance.

Acknowledgements

for their assistance in conducting field monitoring. Comments from two anonymous reviewers were very helpful in improving the manuscript.

References

Allison, G.B., Gee, G.W., Tyler, S.W., 1994. Vadose-zone techniques for estimating groundwater recharge in arid and semiarid regions. Soil Science Society of America Journal 58, 6–14.

Batnasan, N., 2003. Freshwater issues in Mongolia, Proceeding of the National Seminar on IRBM in Mongolia. 24–25 September 2003, Ulaanbaatar, 53–61.

Betts, A.K., Ball, J.H., Beljaars, A.C., Miller, M.J., Viterbo, P.A., 1996. The land surface-atmosphere interaction: a review based on observational and global modeling perspectives. Journal of Geophysical Research 101 (D23), 7209–7225.

Bradley, R.S., 1999. Paleoclimatology: Reconstructing Climates of the Quaternary, second ed. Academic Press, San Diego.

Brutsaert, W., 1982. Evaporation into the Atmosphere: Theory, History and Applications. Kluwer Academic Pub., Boston.

Brutsaert, W., Chen, D., 1996. Diurnal variation of surface fluxes during through drying (or sever drought) of natural prairie. Water Resources Research 32, 2013–2019.

Chase, T.N., Pielke, R.A., Knaff, J., Kittel, T., Eastman, J., 2000. A comparison of regional trends in 1979–1997 depth-averaged tropospheric temperatures. International Journal of Climatology 20, 503–518.

Crago, R.D., 1996. Comparison of the evaporative fraction and the Priestly Taylor α for parameterizing daytime evaporation. Water Resources Research 32, 1403–1409.

Davies, J.A., Allen, C.D., 1973. Equilibrium, potential and actual evaporation from cropped surfaces in southern Ontario. Journal of Applied Meteorology 12, 649–657.

Gee, G.W., Hillel, D., 1988. Groundwater recharge in arid regions: review and critique of estimation methods. Hydrological Processes 2, 255–266.

Hansen, J., Ruedy, R., Gloscoe, J., Sato, M., 1999. GISS analysis of surface temperature change. Journal of Geophysical Research 104, 30997–31022.

Kaihotsu, I., Yamanaka, T., Oyunbaatar, D., Hirata, M., Oishi, K., Muramatsu, K., Miyazaki, S., Kondoh, A., Koike, T., 2002. Preliminary ground-based observation for the soil moisture measurement validation of ADEOS II-AMSR/AMSR-E. Proceedings of the Third Workshop on Remote Sensing of Hydrological Processes and Applications. pp. 1–6.

Kondoh, A., Kaihotsu, I., 2003. Preliminary analysis on the relationship between vegetation activity and climatic variation in Mongolia. Journal of Arid Land Study 13, 147–151.

Malek, E., 2003. Microclimate of a desert playa: evaluation of annual radiation, energy, and water budgets components. International Journal of Climatology 23, 333–345.

Malek, E., Bingham, G.E., 1993. Comparison of the Bowen ratio-energy balance and the water balance methods for the measurement of evapotranspiration. Journal of Hydrology 146, 209–220.

Malek, E., Bingham, G.E., McCurdy, G.D., 1990. Evapotranspiration from the margin and moist playa of a closed desert valley. Journal of Hydrology 120, 15–34.

Malek, E., Bingham, G.E., Or, D., McCurdy, G., 1997. Annual mesoscale study of water balance in a Great Basin heterogeneous desert valley. Journal of Hydrology 191, 223–244.

Miyazaki, S., Yasunari, T., Miyamoto, T., Kaihotsu, I., Davaa, G., Oyunbaatar, D., Natsagdorj, L., Oki, T., 2004. Agrometeorological conditions of grassland vegetation in central Mongolia and their impact for leaf area growth. Journal of Geophysical Research 109, D22106.

Monteny, B.A., Lhomme, J.P., Chehbouni, A., Troufleau, D., Amadou, M., Sicot, M., Verhoef, A., Galle, S., Said, F., Lloyd, C.R., 1997. The role of the Sahelian biosphere on the water and the CO_2 cycle during the HAPEX-Sahel Experiment. Journal of Hydrology 188-189, 516–535.

Ni, J., 2003. Plant functional types and climate along a precipitation gradient in temperate grasslands, north-east China and south-east Mongolia. Journal of Arid Environments 53, 501–516.

Nichols, W.E., Cuenca, R.H., 1993. Evaluation of the evaporative fraction for parameterization of the surface energy balance. Water Resources Research 29, 3681–3690.

Roberts, N., 1994. The Changing Global Environment. Blackwell Publ., Cambridge.

Scanlon, B.R., Tyler, S.W., Wierenga, P.J., 1997. Hydrologic issues in arid, unsaturated systems and implications for contaminant transport. Reviews in Geophysics 35, 461–490.

Sellers, P.J., Dickinson, R.E., Randall, D.A., Betts, A.K., Hall, F.G., Berry, J.A., Collatz, G.J., Denning, A.S., Mooney, H.A., Nobre, C.A., Sato, N., Field, C.B., Henderson-Sellers, A., 1997. Modelling the exchanges of energy, water, and carbon between continents and the atmosphere. Science 275, 502–509.

Shuttleworth, W.J., 1991. Evaporation models in hydrology. In: Schmugge, T.J., Andre, J.-C. (Eds.), Land Surface Evaporation: Measurement and Parameterization. Springer, New York.

Si, J.H., Feng, Q., Zhang, X.Y., Liu, W., Su, Y.H., Zhang, Y.W., 2005. Growing season evapotranspiration from *Tamarix ramosissima* stands under extreme arid conditions in northwest China. Environmental Geology 48, 861–870.

Sneath, D., 1998. State policy and pasture degradation in Inner Asia. Science 281, 1147–1148.

Xue, Y., 1996. The impact of desertification in the Mongolian and the Inner Mongolian grassland on the regional climate. Journal of Climate 9, 2173–2189.

Wraith, J.M., Or, D., 1999. Temperature effects on soil bulk dielectric permittivity measured by time domain reflectometry: experimental evidence and hypothesis development. Water Resources Research 35, 361–369.

Yamanaka, T., Kaihotsu, I., Oyunbaatar, D., 2003. Temperature effect of soil water content measured by time domain reflectometry and its correction using in situ data. Journal of Japan Society of Hydrology & Water Resources 16, 246–254.

Yatagai, A., Yasunari, T., 1995. Interannual variations of summer precipitation in the arid/semi-arid regions in China and Mongolia: their regionality and relation to the Asian summer monsoon. Journal of Meteorological Society of Japan 73, 909–923.